Electrochemical performances of nanostructured anatase TiO_2 synthesized by pulsed high-voltage discharge

UDC 661.882'022-14:541.13

D. P. Opra, *Head of Power Sources Group[1], e-mail: ayacks@mail.ru*
S. V. Gnedenkov, *Deputy Director, Head of Department of Electrochemical Systems and Surface Modification Processes[1], e-mail: svg21@hotmail.com*
V. G. Kuryavyy, *Senoir Researcher of the Laboratory of Fluoride Materials[1]*
S. L. Sinebryukhov, *Head of Nonstationary Surface Processes Laboratory[1]*

[1] Institute of Chemistry of Far Eastern Branch of Russian Academy of Sciences, Vladivostok, Russia.

At present Li-ion batteries have long been used as power supply for a large scale of portable high-technology equipment, such as mobile phones, notebooks, e-books, pads, photo- and video cameras, smartphones, etc. Technological progress puts high requirements on Li-ion batteries performance parameters, including the capacity, power, reliability, storage life, and safety. It should be noted that the safety of modern Li-ion batteries is quite insufficient (because of the high reactivity of lithiated carbon) for using them as power supply modules consisting of a large number of cells. Titania is a more suitable anode material for safe Li-ion batteries due to its higher lithiation-delithiation voltage as compared to graphite. Among the titania polymorphs the anatase TiO_2 is intensively investigated as Li-ion battery anode. In the present paper nanostructured anatase TiO_2 has been synthesized by a facile original method of pulsed high-voltage discharge. As-prepared titania consists of a rough surface of particles having dimensions up to 500 nm composed from nanoparticles with diameters lower than 100 nm. Electrochemical properties of nanostructured anatase TiO_2 nanostructure have been investigated in order to design the anode for Li-ion battery with high capacity and long-life performance. The galvanostatic discharge-charge cycling of the titania electrode vs. Li^+/Li at 0.1C-rate in the range from 3 to 1 V yields approximately 155 $mAh \cdot g^{-1}$ after 20 cycles. The irreversible capacity loss is determined by both lithium intercalation into irreversible sites and decomposition of the electrolyte and the formation of the solid electrolyte interphase layer. The electrochemical reaction mechanism between the Li^+ and anatase TiO_2 has been investigated by the cyclic voltammetry. The obtained results show suitability of the method of pulsed high-voltage discharge for preparing of the nanostructured anode-active materials for Li-ion batteries.

Key words: Li-ion battery, anode, nanostructured material, anatase, titania, irreversible capacity, safety.

DOI: *http://dx.doi.org/10.17580/nfm.2016.01.03*

Introduction

Li-ion batteries (LIB) have widely used as a power sources for portable devices (tablets, smartphones, photocameras, etc.), electric tools, and medical instruments. However, the application of LIBs for hybrid and electric vehicles, uninterruptible power supplies, unmanned underwater vehicles, etc. depends on designing of new, efficient electrode materials [1–5]. The conventional carbonaceous anode material of LIB is characterized by availability, insignificant volume changes (9–10%) during cycling, and theoretical capacity of 372 $mAh \cdot g^{-1}$. At the same time, the practical capacity of carbonaceous anode does not exceed 250–300 $mAh \cdot g^{-1}$. In addition, the safety of conventional LIB due to the extremely strong reactivity of lithiated graphite is not enough for their using as large-size modulus includes a great number of cells. Therefore, nowadays, the synthesis of anode materials having high specific capacity, free from poison, stable during cycling, and reliable safety comprises a topical issue of the basic science [6–8].

Nanostructured Ti-based materials, such as $Li_4Ti_5O_{12}$, TiO_2, $TiOF_2$, etc. are of great interest as an anode materials for safe LIBs due to their higher Li^+ intercalation-deintercalation voltage (>1 V vs. Li^+/Li) [9–11]. Note that lithium titanate $Li_4Ti_5O_{12}$ is the almost commercialized Ti-based anode material at present. However, $Li_4Ti_5O_{12}$ limited capacity of 175 $mAh \cdot g^{-1}$ results in impossibility of its use for high energy density applications such as hybrid and electric vehicles, unmanned underwater vehicles, emergency uninterruptible power supplies, energy storage technologies for renewable power systems, etc. [6, 9]. On the other hand, the theoretical specific capacity of TiO_2 reaches 335 $mAh \cdot g^{-1}$. Among the titania polymorphs the anatase TiO_2 are intensively investigated as LIB anodes due to smaller volume changes (less than 4%) during cycling and higher power density [9, 10]. At the same time, anatase TiO_2 is characterized by low Li-ion diffusivity (10^{-15}–10^{-9} $cm^2 \cdot s^{-1}$) that deteriorates the reversible capacity and rate capability [12–15]. It is well known, that nanostructuring facilitates the Li^+ ions diffusion during the battery cycling [16, 17]. However, most reported preparation routes are unprofitable for nanostructured anatase TiO_2, inconvenient and unsafe in environmental terms. Thus, the development of facile original approaches for synthesis of nanostructured anatase TiO_2 is a great interest [18–20].

In this paper, we report a pulsed high-voltage discharge method for synthesis of nanostructured TiO_2 in the anatase polymorph. The suitability of as-prepared titania as anode material for LIB was investigated by discharge-charge cycling and cyclic voltammetry.

Experiment

Titania was synthesized in plasma by pulsed high voltage discharge in the course of destruction of titanium electrodes and polytetrafluoroethylene wire. In a typical synthesis, Ti electrodes with diameter of 1 mm were located at a distance of 3 mm between them at ambient conditions. High voltage pulsed signal with amplitude of 9 kV, a pulse duration of 100 μs, and a pulse-repetition frequency of 2000 Hz was applied from an external power supply. As a result, the plasma filament emerged between titanium electrodes. The intensive generation of gas-vapor phase was observed after introduction of polytetrafluoroethylene rod into the plasma of pulsed high-voltage discharge. Light grey TiO_2 and $TiOF_2$ composite powder was obtained by a condensation of gas-vapor phase on a surface of quartz substrate. Finally, the as-synthesized composite was heated up to 450 °C at a slow rate of 1.5 °C·min^{-1} using Nabertherm B180 (Germany) muffle furnace and maintained at this temperature for 2 h to prepare of TiO_2 in the anatase polymorph [21–23].

The crystal structure was characterized by *X*-ray powder diffraction (XRD) on Bruker D8-Advance (Germany) diffarctometer with CuK_α-radiation. Identification of the experimental data was performed using the EVA program with the PDF-2 (2006) powder database. The surface morphology was analyzed by scanning electron microscopy (SEM) using Hitachi S5500 (Japan) device, which was combined with energy dispersive *X*-ray (EDX) analyzer.

The working electrode consisted of the anatase TiO_2 (active material), carbon black (electroconductive additive), and polyvinylidene fluoride (binder) at a weight ratio of 80:10:10. The mixture was homogenized in *N*-methylpyrrolidone solvent with use IKA C-MAG HS 7 (China) magnetic stirrer for 12 h at a rate of 250 rpm to prepare uniform viscous slurry. The slurry was spread on a Cu current collector by the doctor blade technique using MTI AFA-I (USA) instrument. The electrode sheet was dried at 60 °C for 24 h in MTI DZF-6020-110P (USA) vacuum oven. Finally, MTI T06 (USA) tool was applied for manually operated cutting of round discs from electrode sheet. The mass of the active material was approximately 5 mg·cm^{-2}. The thickness of the working electrode was equal to 70 μm.

The half-cell was assembled in Plas-Labs 890-NB glove box (USA) under the dry argon atmosphere. Swagelok-type MTI STC-19 (USA) two-electrode cell was used for study of the electrochemical performances. A lithium metal disc with a thickness of 0.1 mm was used as both counter and reference electrode. 1 M solution of $LiBF_4$ salt in the mix of propylene carbonate and dimethoxyethane at a volume ratio of 3:1 was used as an electrolyte. To prevent short circuit a polypropylene separator was used. Relaxation of half-cell was performed for at least 5 h to stabilize the open-circuit voltage. The electrochemical performance was investigated using a Solartron 1470E (UK) potentiostat/galvanostat. The parameters were measured by the galvanostatic discharge-charge technique in the range from 3 to 1 V at current density of 0.1C (C = 335 mA·g^{-1}) during 20 cycles. In this work, due to half-cell applying the lithiation process corresponds to discharge, while the delithiation relates to charge. Cyclic voltammetry (CV) was performed at a scan rate of 0.1 mV·s^{-1} between 3 and 1 V. The measurements were carried out at least on three half-cells for each test.

Results and discussions

The XRD pattern of as-synthesized titania is shown in Fig. 1. All the peaks can be well indexed to anatase with a tetragonal structure (JSCD № 00-021-1272, space group I41/amd). No other peaks were observed on the pattern, indicating high purity of the as-prepared anatase TiO_2. The lattice parameters are found to be $a = b = 3.785$ Å and $c = 9.513$ Å. The anatase structure consists of distorted TiO_6 octahedra sharing two adjacent edges so that infinite planar double chains are formed [24, 25]. There are two types of empty sites (octahedral and tetrahedral) available for hosting foreign ions like lithium. At the same time, the space between TiO_6 is nearly sufficient for Li^+ ions intercalation only into the octahedral vacancies [24, 25]. The anatase unit cell includes the four octahedral sites and occupancy of all of them leads to a formation of tetragonally distorted rock-salt like structure $LiTiO_2$.

The SEM images (Fig. 2) for as-synthesized anatase TiO_2 reveals that the particle surface is relatively rough and apparently built from tiny nanoparticles with diameters lower than 100 nm (Fig. 2, *a*). The nanoparticles are organizing the larger agglomerates having dimensions up to 500 nm (Fig. 2, *b*). According to the EDX results, Ti (38% (at.)) and O (52% (at.)) are uniform distributed on the surface of particles. Except C (10% (at.)) associated with the polytetrafluoroethylene destruction, no other elements have been detected by EDX (Fig. 2, *c*).

The discharge-charge profiles for nanostructured anatase TiO_2 vs. Li^+/Li at a 0.1C-rate are shown in Fig. 3. In accordance with [24–26] the typical voltage

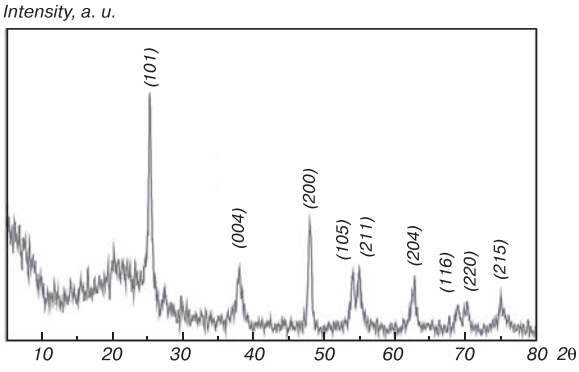

Fig. 1. XRD pattern for as-synthesized anatase TiO_2

plateaus at 1.7 and 1.9 V on discharge and charge curves, respectively, are associated with the Li^+ ions insertion and extraction:

$$xLi^+ + xe^- + TiO_2 \leftrightarrow Li_xTiO_2,$$

where x ranges from 0 to 1 depending on morphology, composition, and other features of titania. It was shown [24–26] that the reversible electrochemical intercalation of Li^+ ions into anatase structure proceeds through a change of phase from the tetragonal ($x \sim 0.05$ in Li_xTiO_2) to orthorhombic ($x \sim 0.5$ in Li_xTiO_2). Only a half of the available interstitial octahedral sites of anatase can be randomly occupied by Li^+ ions, leading to a total reversible capacity of 168 mAh·g^{-1}.

During the 1st cycle discharge the anatase TiO_2 exhibits a specific capacity of 361 mAh·g^{-1}. Accordingly [26, 27] the nanostructuring of anatase TiO_2 enhances its lithium storage capacity up to 335–400 mAh·g^{-1} during the 1st lithiation and to 150–180 mAh·g^{-1} in the subsequent discharge-charge cycles (only at low current densities) due to a shorter diffusion length for both electrons and ions, as well as a larger electrode/electrolyte contact area, which facilitate the Li^+ insertion and extraction. During the 1st charge cycle (Li^+ ions deintercalation) the voltage continuously increases with a flat region at 1.9 V. The specific capacity of 230 mAh·g^{-1} corresponds to relatively low Coulombic efficiency of approximately 64% and large irreversible capacity of 131 mAh·g^{-1}. In accordance with [28, 29] the irreversible capacity is determined by the lithium intercalation into irreversible sites and in a lesser degree by the decomposition of the electrolyte and the formation of the solid electrolyte interphase (SEI) layer.

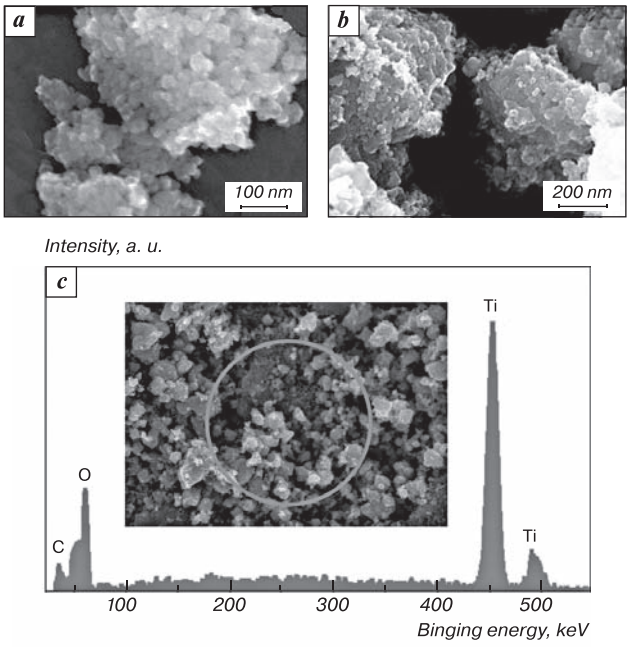

Fig. 2. SEM images at different magnification (*a*, *b*) and EDX spectrum (*c*) for as-prepared anatase TiO_2

Galvanostatic discharge curve of the 2nd cycle for anatase TiO_2 is differed from the 1st cycle curve. At the same time, the charge curves of the 1st and 2nd cycles are closer each other. The 2nd discharge capacity of titania is equal to 211 mAh·g^{-1} (insertion of 0.6 Li^+ into the TiO_2 structural unit). The subsequent charge capacity of 195 mAh·g^{-1} is showed the low irreversible loss and higher Coulombic efficiency for the 2nd cycle.

The cycle performance for anatase TiO_2 electrode vs. Li^+/Li at a 0.1*C*-rate in the voltage range of 3–1 V is demonstrated in Fig. 4, *a*. During the 20-fold cycling the lithiation-delithiation capacities gradually decreasing. However, the capacity fading is more pronounced from the

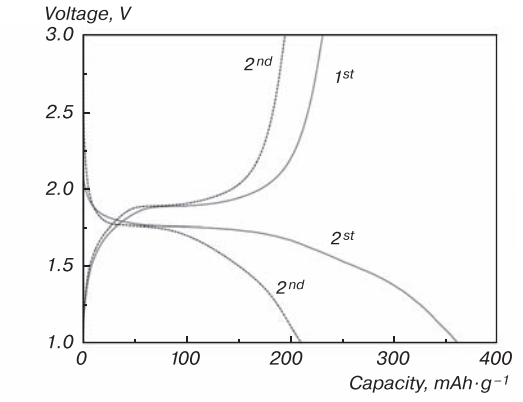

Fig. 3. The 1st and the 2nd cycle's voltage profiles at 0.1*C*-rate for anatase TiO_2 electrode

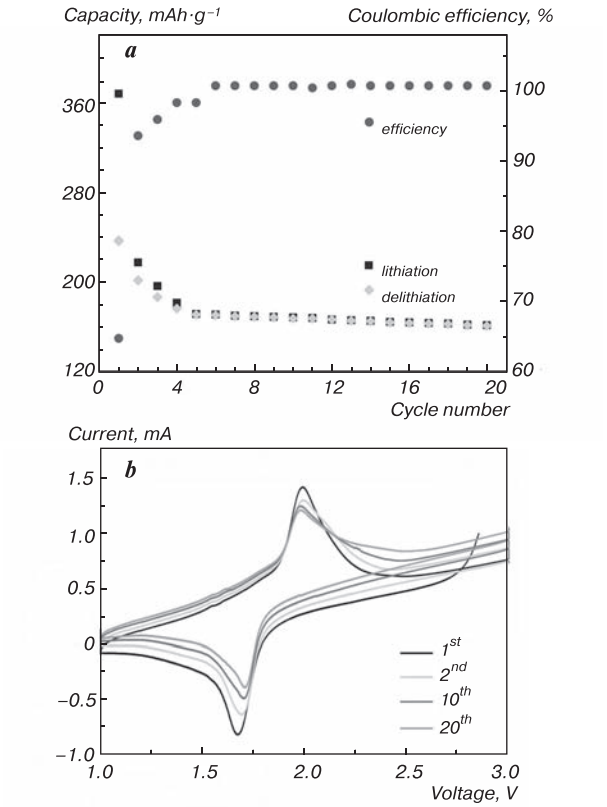

Fig. 4. Cycling performance with a current rate of 0.1*C* (*a*) and cyclic voltammograms recorded at a scan rate of 0.1 mV·s^{-1} (*b*) for anatase TiO_2 electrode

1st to 3nd cycle that attributed by completion of the structural ordering and the SEI formation. The Coulombic efficiency more than 99% is realized after the 3th cycle and the capacity fading rate is estimated to be less than 1% per cycle for the subsequent discharge-charge. After the 20th cycles the reversible capacity is equal to 155 mAh·g^{-1} that is corresponds to 0.45 Li^+ per titania structural unit. The cycling data suggest that the nanostructured anatase TiO_2 synthesized by pulsed high-voltage discharge method is highly stable during lithiation-delithiation.

Cyclic voltammograms for anatase TiO_2 electrode scanned at a rate of 0.1 mV·s^{-1} are shown in Fig. 4, *b*. The CVs is typical for the reversible process [14–16]. For the 1st cycle, in the cathodic polarization process the peaks corresponding to the insertion of Li^+ ions into anatase TiO_2 appear at 1.7 V. The peak at 1.9 V in the following anodic polarization is attributed to Li^+ ions extraction from crystal lattice. During the 2nd cycle, the positions of both cathodic and anodic peaks are slightly changed. Furthermore, some disappearance of peaks is observed due to the irreversible Li^+ insertion, leading to irreversible capacity loss. For the 10th and 20th cycles the tendency are remained, however, the tempo of changes is slowing down. The CV results are in good accordance with the galvanostatic discharge-charge cycling of titania vs. Li^+/Li.

Conclusions

A new concept for synthesis of the nonostructured transition metal oxides had been suggested. In particular, it was found that the anatase TiO_2 *prepared by the method of pulsed high-voltage discharge is a promising anode material for* Li-*ion battery. The as-synthesized titania consisted of nanoparticles with diameter lower than 100 nm, which are collected in agglomerates having dimensions up to 500 nm. 20-fold galvanostatic discharge-charge cycling shows that the specific capacity for nonostructured anatase* TiO_2 i*s equal to 155 mAh·g^{-1}. Cycling efficiency is good, as well as the capacity retention on cycling after an irreversible capacity on the first cycle. The Coulombic efficiency is more than 99%. The synthesis route is original and facile, and could be used to prepare of other nanostructured transition metal oxide anode materials for Li-ion batteries.*

This work was supported by the Russian Science Foundation (grant № 14-33-00009) and Russian Government (Federal Agency of Scientific Organizations). For helpful discussions the authors are grateful to Dr. T. A. Kaidalova from Institute of Chemistry of FEB RAS.

References

1. Xu W., Wang Z., Guo Z., Liu Y., Zhou N., Niu B., Shi Z., Zhang H. J. Power Sources. 2013. Vol. 232. pp. 193–198.

2. Tsivadze A. Yu., Kulova T. L., Skundin A. M. Prot. Met. Phys. Chem. 2013. Vol. 49. pp. 145–150.

3. Madej E., Mantia F. L., Mei B., Klink S., Muhler M., Schuhmann W., Ventosa E. J. Power Sources. 2014. Vol. 266. pp. 155–161.

4. Makaev S. V., Ivanov V. K., Polezhaeva O. S., Tretyakov Yu. D., Kulova T. L., Skundin A. M., Brylev O. A. Russ. J. Inorg. Chem. 2010. Vol. 55 (7). pp. 991–994.

5. Churikov A. V., Ivanishchev A. V., Ivanishcheva I. A., Zapsis K. V., Gamayunova I. M., Sycheva V. O. Russ. J. Electrochem. 2008. Vol. 44. pp. 530–542.

6. Marom R., Amalraj S. F., Leifer N., Jacob D., Aurbach D. J. Mater. Chem. 2011. Vol. 21. pp. 9938–9954.

7. Tarascon J.-M., Armand M. Nature. 2001. Vol. 414. pp. 359–367.

8. Kulova T. L., Pleskov Yu. V., Skundin A. M., Terukov E. I., Konkov O. I. Russ. J. Electrochem. 2006. Vol. 42 (7). pp. 708–714.

9. Dylla A. G., Henkelman G., Stevenson K. J. Accounts Chem. Res. 2013. Vol. 46 (5). pp. 1104–1112.

10. Wagemaker M., Van Well A. A., Kearley G. J., Mulder F. M. Solid State Ionics. 2004. Vol. 175. pp. 191–193.

11. Opra D. P., Gnedenkov S. V, Sokolov A. A., Zheleznov V. V., Voit E. I., Sushkov Yu. V., Sinebryukhov S. L. Scripta Mater. 2015. Vol. 107. pp. 136–139.

12. Amarilla J. M., Morales E., Sanz J., Sobrados I., Tartaj P. J. Power Sources. 2015. Vol. 273. pp. 368–374.

13. Kulova T. L. Russ. J. Electrochem. 2013. Vol. 49. pp. 1–25.

14. Rahman M. A., Wang X., Wen C. J. Energ. Chem. 2015. Vol. 24. pp. 157–170.

15. Li G., Zhang Z., Peng H., Chen K. RSC Advances. 2013. Vol. 3. pp. 11507.

16. Sinebryukhov S. L., Opra D. P., Gnedenkov S. V., Minaev A. N., Sokolov A. A., Kuryavyi V. G., Zheleznov V. V. Int. Ocean Polar Eng. 2015. Vol. 1. pp. 621–628.

17. Wu F., Li X., Wang Z., Guo H., Wu L., Xiong X., Wang X. J. Alloy. Compd. 2011. Vol. 509. pp. 3711–3715.

18. Ivanov V. K., Fedorov P. P., Baranchikov A. Y., Osiko V. V. Russ. Chem. Rev. 2014. Vol. 83. pp. 1204–1222.

19. Zeng Y., Zhang W., Xu C., Xiao N., Huang Y., Yu D. Y. W., Hng H. H., Yan Q. Chem. Eur. J. 2012. Vol. 18. pp. 4026–4030.

20. Gnedenkov S. V, Opra D. P., Zheleznov V. V., Sinebryukhov S. L., Voit E. I., Sokolov A. A., Sushkov Yu. V., Podgorbunsky A. B., Sergienko V. I. Russ. J. Inorg. Chem. 2015. Vol. 60 (6). pp. 658–664.

21. Gnedenkov S. V., Opra D. P., Sinebryukhov S. L., Kuryavyi V. G., Ustinov A. Yu., Sergienko V. I. J. Alloy. Compd. 2015. Vol. 621. pp. 364–370.

22. Kuryavyi V. G., Ustinov A. Yu., Opra D. P., Zverev G. A., Kaidalova T. A. Mater. Lett. 2014. Vol. 137. pp.398–400.

23. Gnedenkov S. V., Opra D. P., Kuryavyi V. G., Sinebryukhov S. L., Ustinov A. Yu., Sergienko V. I. Nanotechnol. Russ. 2015. Vol. 10(5/6). pp. 353–356.

24. Koudriachova M. V., Harrison N. M., De Leeuw S. W. Solid State Ionics. 2002. Vol. 152/153. pp. 189–194.

25. Koudriachova M. V., Harrison N. M. J. Mater. Chem. 2006. Vol. 16. pp. 1973–1977.

26. Jiang C., Zhang J. J. Mater. Sci. Technol. 2013. Vol. 29(2). pp. 97–122.

27. Ren Z., Chen C., Fu X., Wang J., Fan C., Qian G., Wang Z. Mater. Lett. 2014. Vol. 117. pp. 124–127.

28. Chen L., Laif S., Nie P., Zhang X., Li H. Electrochim. Acta. 2012. Vol. 62. pp. 408– 415.

29. Kulova T. L., Skundin A. M. Russ. J. Electrochem. 2012. Vol. 48(3). pp. 330–335.

NFM